We are IntechOpen,
the world's leading publisher of
Open Access books
Built by scientists, for scientists

6,900
Open access books available

186,000
International authors and editors

200M
Downloads

Our authors are among the

154
Countries delivered to

TOP 1%
most cited scientists

12.2%
Contributors from top 500 universities

CLARIVATE ANALYTICS
BOOK CITATION INDEX
INDEXED

WEB OF SCIENCE™

Selection of our books indexed in the Book Citation Index
in Web of Science™ Core Collection (BKCI)

Interested in publishing with us?
Contact book.department@intechopen.com

Numbers displayed above are based on latest data collected.
For more information visit www.intechopen.com

Immobilized redox proteins: mimicking basic features of physiological membranes and interfaces

Daniel H. Murgida, Peter Hildebrandt and Smilja Todorovic
INQUIMAE, University of Buenos Aires - CONICET,
Argentina,
Technische Universität Berlin,
Germany,
ITQB, The New University of Lisbon,
Portugal

1. Introduction

Redox proteins perform diverse functions in cells, including electron transport, energy conversion, detoxification, enzymatic catalysis, signalling and gene regulation. The evolutionary optimised specificity and efficiency of enzymes has stimulated attempts to exploit these biocatalysts for a variety of technological applications. For example, enzymes are nowadays used to promote or to detect bio-specific interactions in biosensors (Karube, 1989). Several generations of low cost glucose oxidase–based biosensors are commercially available for monitoring the levels of glucose in diabetic individuals (Henning and Cunningham, 1998). Peroxidases are employed for biosensing of hydrogen peroxide and phenolic compounds, being relevant in environmental, pharmaceutical, clinical and industrial applications (Arya *et al.*, 2009). Cytochromes P450 possess a high potential as biocatalysts for chemical synthesis although the transfer to biotechnological applications still represents a challenge (Leland and Clark, 1989; Todorovic *et al.*, 2006; Cass, 2007).

Understanding the enzymatic processes in cellular systems as well as in technological devices strongly depends on the knowledge of the molecular functioning of the enzymes. To this end specific approaches have been designed to explore the molecular processes of enzymes and redox proteins under conditions that reproduce most closely the physiological reaction. Membrane–bound redox proteins, such as respiratory chain electron transfer (ET) complexes, are incorporated into phospholipid bilayers, thus exerting their function in a hydrophobic environment under influence of the membrane potential. Small soluble metalloproteins that shuttle electrons between ET enzymes interact with the membrane-bound redox partners and the membrane itself. As a result of these interactions, the ET processes of electron shuttles are also subjected to strong electric fields at the membrane-solution interface. These conditions are difficult to reproduce experimentally. In this respect, immobilization of redox proteins on biocompatible metal supports that function as

electrodes represents a powerful alternative, allowing application of direct electrochemistry and surface-enhanced vibrational spectroelectrochemical techniques. These methods permit determination of kinetic and thermodynamic parameters of the heterogeneous ET in a protein that is exposed to physiologically relevant electric fields. Furthermore, ET steps can be controlled in terms of directionality, distance, and driving force. In addition, spectroelectrochemical methods can simultaneously probe the active site structure and conformational dynamics concomitant to the ET.

In this chapter we will present an overview of recent developments in the field of biocompatible immobilization of membrane-bound and soluble redox proteins on metal electrodes, and of the spectroelectrochemical techniques used for the *in situ* characterization of the structure, thermodynamics and reaction dynamics of the immobilized proteins.

After a brief description of biological ET chains and their constituting complexes (Section 2), we will introduce some of the strategies for protein immobilization (Section 3), with special emphasis on self-assembled monolayers (SAMs) of functionalized alkanethiols as versatile biocompatible coatings that can be tailored according to the specific requirements. In Section 4 we will describe the basic principles of stationary and time-resolved surface-enhanced vibrational spectroscopies (SERR and SEIRA) as valuable tools for studying specifically the redox centres or the immobilized metalloproteins. The contents of the first 3 sections are integrated in Section 5, where recent progress in the immobilization and SERR/SEIRA characterization of different components of ET respiratory chains, mainly oxygen reductases and cytochromes will be discussed. We will conclude with a brief outlook (Section 6).

2. Redox proteins under physiological conditions

In this section we will provide a brief introduction to the complex ET chains involved in the energetics of organisms, i.e. respiratory and photosynthetic chains. In spite of obvious differences, these two types of systems share a number of common features that must be taken into account when investigating them using biomimetic approaches. First, both types of chains consist of a series of membrane-integrated redox active protein complexes that communicate through hydrophilic (e.g. cytochromes) and hydrophobic (e.g. quinones) electron shuttles. Second, the energy provided by the sequence of exergonic ET events is utilized by some of the constituting membrane proteins for translocating protons across the membrane against an electrochemical gradient. This gradient is, for example, utilized for driving ATP synthesis. Common to components of both ET chains are the specific reaction conditions that deviate substantially from redox processes of proteins in solution. Characteristic features are the restricted mobility of the membrane integral and peripheral proteins and the potential distribution across the membrane that displays drastic changes in the vicinity of the lipid head groups, giving origin to strong local electric fields.

2.1 Electron transfer chains

Membranes are essential in cells for defining structural and functional features, controlling intracellular conditions and responding to the environment. They permit maintaining the non-equilibrium state that keeps cells alive. Phospholipids are the main components of cell membranes, responsible for the membrane shape and flexibility. They are self-assembled in such a manner that non-polar acyl chains driven by hydrophobic interactions orient themselves towards the center of the membrane, while the polar groups remain exposed to the

solution phase, e.g., the cytoplasm and periplasm. The constituent phospholipids, which are typically asymmetrically distributed along the membrane, differ between cellular and mitochondrial membranes. Similar to smectic liquid crystals, membranes present continuous, ordered and oriented, but inhomogeneous structures (Gennis, 1989; Hianik, 2008).

A large variety of proteins are incorporated into or associated to membranes, including enzymes, transporters, receptors and structural proteins. Enzymes are the most abundant of all membrane proteins. Together with water soluble proteins and lipophilic compounds, membrane-bound enzymes compose ET chains. In eukaryotic organisms the oxidation of nutrients such as glucose and fatty acids produces reduced metabolites, namely NADH and succinate, which upon oxidation deliver electrons though ET chains to molecular oxygen. ET occurs through a series of sequential redox reactions between multisubunit transmembrane complexes (Figure 1), situated in the inner mitochondrial membrane of non-photosynthetic eucaryotic cells, or in the cytoplasmatic (cell) membrane of bacteria and archaea. The complexes involved in a canonical respiratory chain are:

- Complex I (NADH : ubiquinone oxidoreductase or NADH dehydrogenase): catalyzes two-electron transfer from NADH to quinone. It is composed of 46 subunits in eukaryotic complexes, but only of 13 to 14 subunits in bacteria, which ensure the minimal functional unit. Electrons enter the enzyme trough a non-covalently bound FMN primary acceptor and are then passed to the quinone molecules via several iron-sulfur clusters.

- Complex II (succinate : ubiquinone oxidoreductase or succinate dehydrogenase): couples two electron oxidation of succinate to fumarate with reduction of quinone to quinol, by transferring electrons from a covalently bound FAD, via iron-sulfur clusters to heme group(s) located in the transmembrane part of the complex, and ultimately to the quinones.

- Complex III (ubiquinol : Cyt-c oxidoreductase or bc_1 complex): catalyzes the transfer of two electrons from ubiquinol to two Cyt-c molecules. It is composed of 10 to 11 subunits in mitochondria and 3 subunits in cell membranes of bacteria and archaea, which bear all prosthetic groups: two low-spin hemes b, a Rieskie type iron-sulfur cluster and a heme c_1. The last redox center is located near the docking site of the electron acceptor Cyt-c.

- Complex IV (Cyt-c : oxygen oxidoreductase or Cyt-c oxidase): catalyzes reduction of oxygen to water by utilizing four electrons received from four molecules of Cyt-c, or alternative electron donors present in some bacteria and archaea (see below).
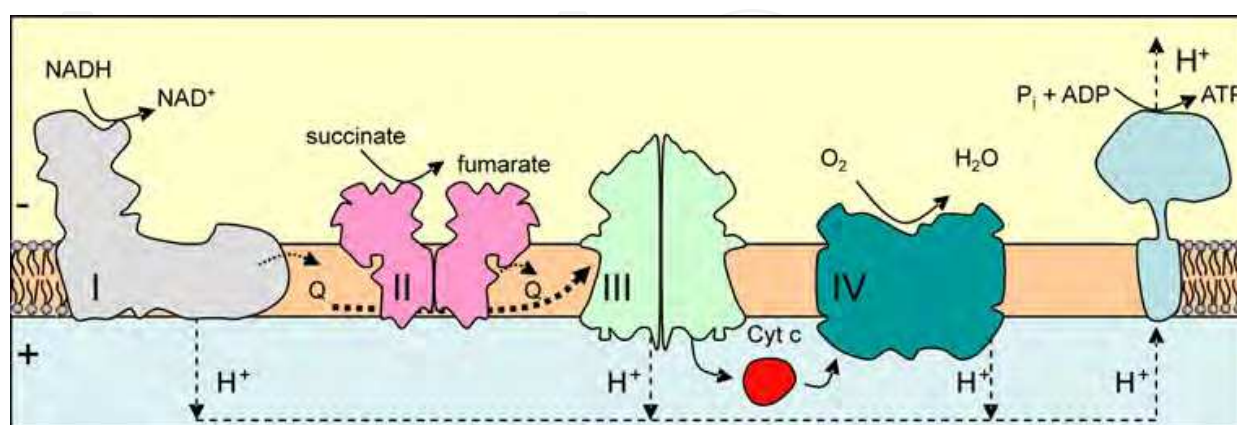

Fig. 1. Schematic representation of the mitochondrial respiratory electron transfer chain. The four complexes (I to IV), and their respective electron transfer reactions are depicted, together with proton fluxes and ATP synthase.

The ET reactions through complexes I, III and IV are coupled to proton translocation across the membrane, contributing to generation and maintenance of a transmembrane electrochemical potential. Protons move back into the mitochondrial matrix (or cytoplasm) through the ATP synthase via an energetically downhill process that provides the energy for the synthesis of ATP.

The eukaryotic photosynthetic ET chain is analogous to the respiratory chain, but structurally and functionally more complex. It is composed of: three multisubunit transmembrane complexes, namely photosystem I, photosystem II and the cytochrome b_6f complex, several soluble electron carriers (e.g. plastocyanin and ferredoxin), lipophilic hydrogen carrier plastoquinone, and light harvesting complexes. The trapping of the light by the two reaction centers (photosystem I and II) results in a charge separation across the stroma (thylakoid) membrane and furthermore in oxidation of water to oxygen by photosystem II. The energy produced by this process serves as the driving force for ET which is, as in respiration, coupled to proton translocation across the membrane and, thus, to the synthesis of ATP. In addition to respiratory and photosynthetic redox enzymes, membrane–bound ET chains also include i) cytochrome P450 containing microsomal and ii) mitochondrial adrenal gland cytochrome P450 systems, that carry out catabolic and anabolic reactions, with fatty acid desaturase and cytochromes P450, respectively, as terminal enzymes (Gennis, 1989).

Bacteria and archaea tend to have simpler ET complexes and more versatile respiratory chains in terms of electron donors and terminal electron acceptors that allow for alternative ET pathways and, therefore, ensure adaptation to different external conditions (Pereira and Teixeira, 2004). The gram negative bacterium *E. coli*, for example, lacks complex III. Instead, the terminal oxygen reductase in its respiratory ET chain is a quinol : oxygen oxidoreductase. Moreover, when growing under aerobic conditions, *E. coli* can express different quinol oxidases to accommodate to the external conditions. In addition to terminal oxygen reductases, it can also employ a wide range of terminal electron acceptors besides oxygen, such as nitrite, nitrate, fumarate or DMSO and express other terminal reductases, accordingly. Similarly, soil bacterium *Paracoccus denitrificans* can fine-tune the expression of the appropriate oxygen reductase (aa_3, cbb_3 or ba_3), depending on the oxygen pressure levels in the surrounding media. Bacteria and archaea also show a high level of diversity in electron carriers, water soluble proteins (Cyt-c, HiPIP, and Cu proteins like sulfocyanin, plastocyanin and amicyanin) and structurally different lipophilic quinones.

The intricate complexity of ET chains implies that understanding their functioning on a molecular level and identification of the factors that govern electro-ionic energy transduction is virtually impossible, unless simplified biomimetic model systems are utilized. The zero-order approximation usually consists of purification of the individual proteins and their characterization by spectroscopic, electrochemical and other experimental methods (Xavier, 2004; Pitcher and Watmough, 2004). This task can be relatively simple for small soluble proteins but significantly more challenging in the case of membrane complexes, due to the typically quite large number of cofactors. The main concern towards studying the membrane components of the redox chains in solution are related to difficulties in reproducing characteristics of the natural reaction environment, governed by the structural and electrical properties of membranes. First, *mobility* of the proteins is *strongly restricted.* Integral membrane proteins are embedded into the lipid bilayer and stabilized by hydrophobic interactions. Their soluble redox partners either bind to the membrane surface or to the solvent exposed part of

the reaction partner. Second, the transition from the non-polar core to the polar surface of the lipid bilayer implies a substantial *variation of dielectric constants*, which imposes specific boundary conditions for the movement and translocation of charges. Third, different ion concentrations on the two sides of the membrane generate transmembrane potential ($\Delta\phi$), which together with the surface (ϕ_s) and the dipole (ϕ_d) potentials contributes to a complex potential profile across the membrane with particularly sharp changes and thus very *high electric field* strengths (up to 10^9 V/m) in the region of charged lipid head groups (Clarke, 2001) (Figure 2). Electric fields of such magnitude are expected to affect the dynamics of the charge transfer processes and the structures of the proteins, thereby resulting in reaction mechanisms that may differ from those observed in solution.
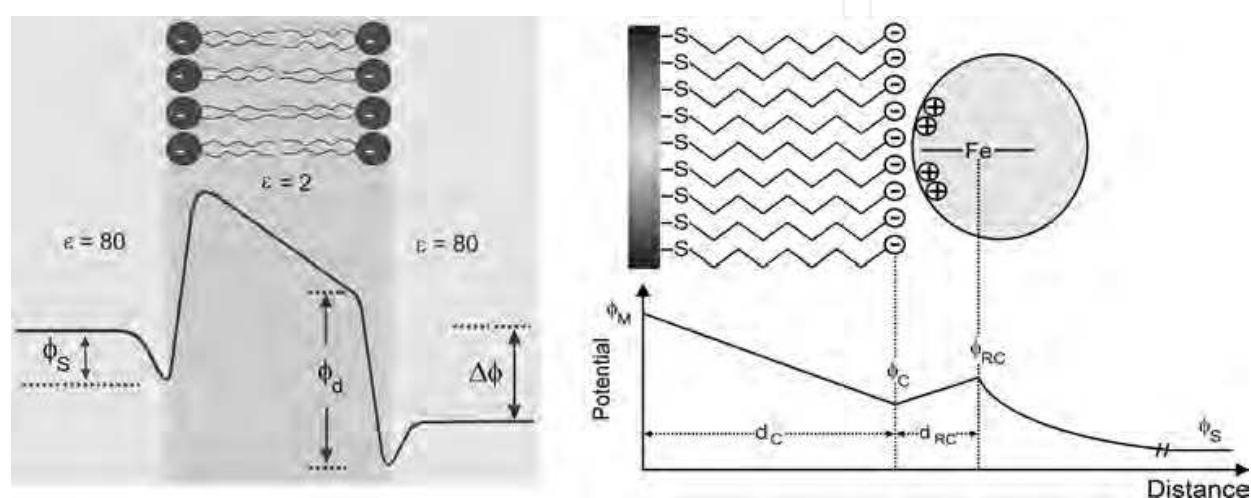

Fig. 2. Schematic representation of the interfacial potential distribution in a lipid bilayer (left) and at a SAM-coated electrode (right).

3. Biocompatible protein immobilization

Immobilization of proteins on solid supports such as electrodes may account for two distinct processes: (i) physical entrapment and (ii) attachment of proteins (Cass, 2007). The former process refers to a thin layer of protein solution trapped by a membrane or a three-dimensional polymer matrix on the solid support, resulting in non-organized and non-oriented protein deposition as, for instance, in sol-gel enzyme electrodes (Gupta and Chaudhury, 2007). The term attachment refers to covalent binding or non-covalent adsorption of the enzyme to the solid surface such as tin, indium and titanium oxide, chemically and electrochemically modified noble metal or carbon electrodes. Adsorption of proteins on bare solid supports often leads to conformational changes or even denaturation. Thus, successful immobilization relies almost exclusively on coated electrodes. Surface coating needs to be well defined in terms of chemical functionalities and physical properties. Self assembled monolayers (SAMs) of alkanethiols are among the most popular biocompatible coatings employed in studies of interfacial interactions for addressing fundamental aspects of heterogeneous ET, but also molecular recognition and cell growth processes, heterogeneous nucleation and crystallization, biomaterial interfaces, etc (Ulman, 2000).

The adsorption of proteins on the conducting, coated surface may be *non-specific* and *non-covalent*, i.e. promoted by electrostatic or van der Waals interactions between the surface functional groups of the modified electrode and amino acid residues of the protein. *Non-covalent* but *specific* interactions, based on molecular recognition, involve affinity coupling between two proteins such as antibody/antigene. This is the most commonly exploited immobilization strategy in the growing field of protein microarrays (Hodneland *et al.*, 2002). Non-covalent and specific interactions also include adsorption of a protein that possesses well defined charged (or hydrophobic) surface patches on a solid surface with opposite charge (or hydrophobic). *Covalent* binding of the protein typically accounts for cross-linking between functional groups of the protein and the surface, using carboxylate, amino or thiol side chains of amino acids on the proteins surface. Specifically, for thiol-based attachments not only natural surface cysteine side chains can be used, but Cys residues can also be introduced at a certain position on the protein surface, in order to control or to modify the attachment site.

Tailoring of novel biocompatible coatings and linkers has been a subject of intense research over the last three decades owing to the importance of protein immobilization under preservation of the native state structure for fundamental and applied purposes. Aiming to the same goal, parallel efforts have been made in the rational design of proteins. Due to the possibility of manipulating DNA sequences and the availability of bacterial expression systems for producing engineered proteins from modified genes, it is now feasible to modify their surface properties in order to promote a particular immobilization strategy (Gilardi, 2004). Such protein modifications may involve introducing of an additional sequence such as a histidine tag, or deleting hydrophobic membrane anchors to produce soluble protein variants.

3.1 Self-assembled monolayers (SAMs) of alkanethiols

Due to the high affinity of thiol groups for noble metals, ω-functionalized alkanethiols spontaneously self-assemble on metal surfaces, forming densely packed monolayers. They are commercially available in a wide variety of functional head groups and chain lengths, allowing fine tailoring of the metal coating by simple immersion of the metal support into a solution of the alkanethiols. A number of physicochemical techniques for surface analysis and spectroscopic characterization of SAMs, such as: Raman spectroscopy, reflectance absorption IR spectroscopy, X-ray photoelectron spectroscopy, high-resolution electron energy loss spectroscopy, near-edge EXAFS, X-ray diffraction, contact-angle goniometry, elipsometry, surface plasmon resonance, surface scanning microscopy, STM and AFM, as well as electrochemical methods, are nowadays routinely used for probing monolayer assembly, structural properties and stability of SAMs (Love *et al.*, 2005). Several factors influence the stability and structure of SAMs, such as solvent, temperature, immersion time, the purity and chain length of the alkanethiols, as well as the purity and the type of the metal. The fast initial adsorption of the alkanethiol molecules, the kinetics of which is governed by surface-headgroup interactions, is followed by a slower rearrangement process driven by inter-chain interactions. Long alkanethiol molecules (n > 10) tend to form more robust SAMs, owing to both, kinetic and thermodynamic factors. The pKa values of acidic or basic ω-functional groups of SAMs differ significantly from those of the amphiphiles in solution. For SAMs with carboxylic head groups the pKa decreases with decreasing chain length. SAMs are electrochemically stable only within a certain range of potentials, which

depends on the chemical composition of the SAM and the type of metal support. Reductive desorption typically occurs at potentials of - 1.00 ± 0.25 V (vs. Ag/AgCl). For a more detailed account on the preparation, tailoring, and characterisation of SAM coatings, the reader is referred to specialised reviews (Ulman, 1996; Love et al., 2005).

3.2 Immobilization of soluble proteins

SAMs of alkanethiols provide a biocompatible interface for the immobilization of proteins on metal electrodes allowing for an electrochemical characterization of the protein under preservation of its native structure. These simple systems can be regarded as biomimetic in the sense that they reproduce some basic features of biological interfaces. The appropriate choice of the alkanthiol head group allows in some cases for specific binding of proteins, Figure 3.

Alkanethiols with pyridinyl head groups may replace the axial Met-80 ligand of the heme in mitochondrial Cyt-c to establish a direct link between the redox site and the electrode (Wei et al., 2002; Murgida et al., 2004b; Murgida and Hildebrandt, 2008). Similarly, apo-glucose oxidase (GOx) was successfully immobilized on a flavin (FAD)-modified metal (Xiao et al., 2003). The carboxyl-terminated SAMs can be activated by carbodiimide derivatives for covalent binding of proteins via the NH_2 groups of Lys surface residues. Several enzymes, like GOx, xanthine oxidase, horse-reddish-peroxidase (HRP), were linked to modified carbon electrodes through formation of amide bond. In each case, the amperometric response of these simple bioelectronic devices could be measured upon detection of glucose, xanthine and hydrogen peroxide, respectively (Willner and Katz, 2000). Carboxylate headgroups can also provide negatively charged surfaces for the electrostatic immobilization of proteins with positively charged surface patches, as it is the case of Cyt-c that possesses a ring-shaped arrangement of positively charged lysine residues, naturally designed for interaction with the redox partners (Murgida and Hildebrandt, 2008). By changing the SAM chain length ET rates can be probed as a function of distance (Murgida and Hildebrandt, 2004a; Todorovic et al., 2006). Furthermore, SAMs permit systematic control of the strength of the interfacial electric field. The potential drop across the electrode/SAM/protein interface, and thus the electric field strength experienced by the immobilized protein, can be described based on a simple electrostatic model (Figure 2) as a function of experimentally accessible parameters. Within this model, the electric field strength E_F at the protein binding site can be described in terms of the charge densities at the SAM surface (σ_C) and at the redox site (σ_{RC}) as well as of the potential drop at the redox site ($E_{RC} = E^0_{ads} - E^0_{sol}$), which increases with the SAM thickness d_c (Equation 1) (Murgida and Hildebrandt, 2001a):

$$E_F(d_C) = \frac{\varepsilon_0 \varepsilon_S \kappa E_{RC} - \sigma_C - \sigma_{RC}}{\varepsilon_0 \varepsilon_C} \qquad (1)$$

where E^0_{ads} and E^0_{sol} are the apparent standard reduction potentials of the protein in the adsorbed state and in solution, respectively, κ is the inverse Debye length, and ε_s and ε_c denote the dielectric constants of the solution and the SAM, respectively. For carboxylate-terminated SAMs, the electric field strength at the Cyt-c binding site is in the order of 10^9 V m^{-1}, which is comparable to the upper values estimated for biological membranes in the

vicinity of charged lipid head groups. Higher field strengths are predicted for phosphonate-terminated SAMs and sulfate monolayers for which $|\sigma_C|$ is distinctly larger. The charge density of the SAM is defined by the pK_a of the acidic head groups in the assembly, which increases with the number of methylene groups, and by the pH of the solution. Thus, the electric field strength at the protein binding site can be varied within the range ca. 10^8-10^9 V m^{-1} by changing the length of the alkanethiols without modifying any other parameter. The strength of the E_F can also be controlled via the electrode potential and the nature of the SAM head group, as well as via the pH and ionic strength of the solution (Murgida and Hildebrandt, 2001a; Murgida and Hildebrandt, 2001b; Murgida and Hildebrandt, 2002; Murgida and Hildebrandt, 2008).
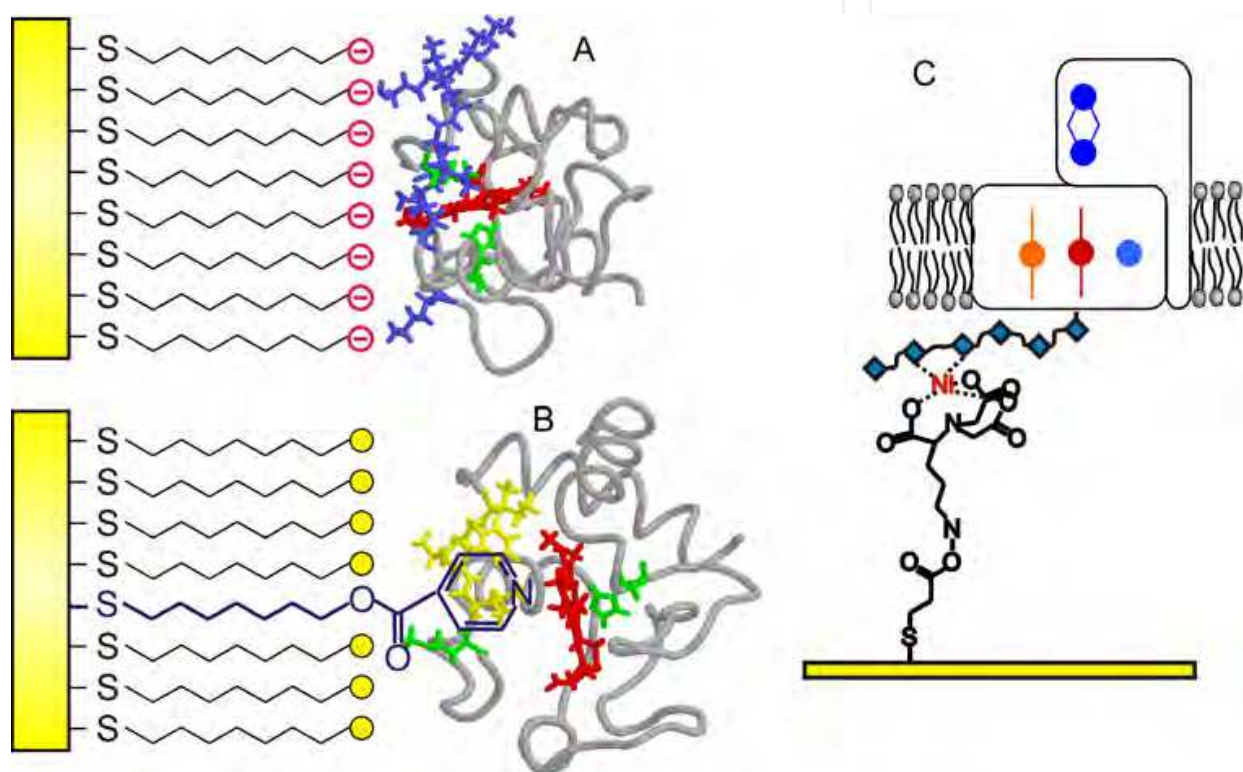

Fig. 3. Schematic representation of some strategies for biocompatible protein binding to metal electrodes: A) electrostatic binding of Cyt-c to a COOH-terminated SAM; B) coordinative binding of Cyt-c to a Py-terminated SAM; C) specific binding of a His-tagged CcO to a Ni-NTA coated electrode.

SAMs can also be formed by hydroxyl-, amino- and methyl-terminated alkanethiols. Hydroxyl-terminated alkanethiols favour polar interactions but may also allow for covalent immobilization (via chlorotriazines and Tyr or Lys amino acid residues) as shown for GOx, ferritin and urease (Willner *et al.*, 2000). Amino–terminated alkanethiols can provide positively charged surfaces for electrostatic binding of proteins rich in surface exposed carboxylic side chains of Asp and Glu, or for cross-linking upon activation of carboxylic groups of the protein (Willner *et al.*, 2000). Methyl-terminated alkanethiols are suitable for immobilization of proteins via hydrophobic interactions (Rivas *et al.*, 2002; Murgida and Hildebrandt, 2008). ´Mixed´ monolayers prepared from alkanethiols with different head-groups in variable molar ratios, provide a surface engineered with gradients of charge,

capable of accommodating proteins with less well defined (or ´diluted´) surface charge distribution via the interplay of different interactions. Mixed SAMs of carboxyl and methyl-terminated alkanethiols were used for HRP immobilization (Hasunuma *et al.*, 2004), while hydroxyl/methyl-terminated SAMs provided the best coating for immobilization of genetically manipulated soluble subunits of *caa*$_3$, *cbb*$_3$, and *ba*$_3$ oxygen reductases, as well as some soluble heme proteins (Ledesma *et al.*, 2007; Kranich *et al.*, 2009). Moreover, the use of mixture of alkanethiols of different chain lengths (and headgroups) may fulfil specific steric requirements of the adsorbate. This strategy has been successfully employed for characterizing the interfacial enzymatic reaction of cutinase by electrochemical methods (Nayak *et al.*, 2007). Other possibilities include mixed SAMs composed of glycol-terminated and biological-ligand-terminated alkanethiols, which appear to be a surface of choice for immobilization of a variety of biomolecules including DNA, carbohydrates, antibodies, and whole bacterial cells that are particularly important for the design and construction of affinity immunosensors (Clarke, 2001; Love *et al.*, 2005; Collier and Mrksich, 2006).

3.3 Immobilization of membrane proteins

Membrane proteins are partially or fully integrated into the lipid bilayer, requiring, therefore, a hydrophobic environment to maintain the native structure and avoid aggregation upon isolation. Besides, they are large, typically composed of several subunits that are often prone to dissociation during the purification process. The structural and functional integrity of the proteins in the solubilized form sensitively depends on the type of detergent used to provide a hydrophobic environment in vitro.

Several models for physiological membranes that display different levels of complexity have been developed, including Langmuir-Blodget (LB) lipid monolayer films (He *et al.*, 1999), bilayer lipid films and liposomes (Hianik, 2008). Protein containing lipid monolayer films formed on solid supports are frequently used for the construction of biosensors. Phospholipid bilayers can be produced in a controllable manner, with tunable thickness, surface tension, specific and electrical capacity. They are the most suitable systems for studies of membrane pores and channels. Liposomes are closed bilayer systems that can be formed spontaneously either from bacterial cell (or mitochondrial) membrane fractions containing the incorporated proteins, or from phospholipids subsequently modified by proteins. They are considered to be good model membranes in studies of transmembrane enzymes involved in coupled reactions on opposite sides of the membrane, as well as proteins involved in solute transport or substrate channeling (Gennis, 1989).

Immobilization strategies for ET membrane proteins have been developed particularly in studies of terminal oxygen reductases. In the simplest approach a detergent-solubilized protein is spontaneously adsorbed on a metal surface. Most likely, immobilization takes place via interactions of the detergent molecules with the layer of specifically adsorbed anions that the metal surface carries above the potential of zero-charge. In fact, the detergent n-dodecyl-β-D-maltoside, commonly used for solubilization of membrane proteins, has been shown to adsorb to these surfaces, providing a biocompatible interface for subsequent protein adsorption under preservation of its structural and functional integrity (Todorovic *et al.*, 2005). This finding is in contrast to the behavior observed for soluble proteins for which the direct adsorption on a bare metal, in the absence of detergent, may cause a (partial) degradation (Murgida and Hildebrandt, 2005). Mixed SAMs composed of CH$_3$ and OH terminated alkanethiols were shown to be a promising choice for immobilization of

detergent-solubilized membrane proteins, such as complex II from *R. marinus* (unpublished data). Direct adsorption of solubilized membrane proteins, however, cannot guarantee a uniform orientation of the immobilized enzyme. In an attempt to overcome this problem, a preformed detergent solubilized Cyt-c/CcO complex was immobilized on Au electrodes coated with hydroxyl-terminated alkanetiols at low ionic strength. It was studied by electrochemical methods, which however, do no permit unambiguous conclusions regarding the enzyme structure and orientation in the immobilized state (Haas *et al.*, 2001). A similar approach was applied to a fumarate reductase immobilized on Au electrode with hydrophobic coating (Kinnear and Monbouquette, 1993).

An alternative immobilization method has been developed for proteins that contain a genetically introduced His tag (Friedrich *et al.*, 2004; Ataka *et al.*, 2004; Giess *et al.*, 2004; Hrabakova *et al.*, 2006; Todorovic *et al.*, 2008). After functionalizing the solid support with Ni (or Zn) NTA (3,3´-dithiobis[N-(5amino-5-carboxy-pentyl)propionamide-N, N´-diacetic acid)] dihydrochloride) monolayer, the protein can be attached via His coordination to the Ni center, Figure 3C. The high affinity of the His tag, inserted into the protein sequence either at N or C terminus, towards Ni-NTA assures large surface coverage of uniformly oriented protein molecules even at relatively high, physiologically relevant ionic strengths. The last immobilization step is the reconstitution of a lipid bilayer from 1,2-diphytanoyl-*sn*-glycero-3-phosphocholine and the removal of the detergent using biobeads. This method was recently employed for immobilization of several oxygen reductases on Au and Ag electrodes. Different steps of the assembly were demonstrated by SEIRA spectroscopy and atomic-force microscopy, providing the evidence for the formation of the lipid bilayer. Moreover, separations of the redox centers from the metal surface in the final biomimetic construct are yet not too large for applying surface enhanced vibrational spectroscopies (Friedrich *et al.*, 2004).

4. Methods for probing the structure and dynamics of immobilized proteins: vibrational spectroscopy

It is clear that the development of novel protein-based bioelectronic devices for basic and applied purposes heavily relies upon design of new biomimetic or biocompatible materials. However, it also requires appropriate experimental approaches capable of monitoring *in situ* the structure and reaction dynamics of the immobilized enzymes under working conditions. These information are crucial for understanding and eventually improving the performance of protein-based devices.

Here we will describe basic principles of SERR and SEIRA spectroelectrochemical techniques, which are among the most powerful approaches for characterization of thermodynamic, kinetic and structural aspects of immobilized redox proteins.

4.1 (Resonance) Raman and infrared spectroscopies

Raman and IR spectroscopies probe vibrational levels of a molecule, providing information on molecular structures. A vibrational mode of a molecule will be Raman active only if the incident light causes a change of its polarizability, while IR active modes require a change in dipole moment upon absorption of light. For molecules of high symmetry, these selection rules allow grouping the vibrational modes into Raman- or / and IR-active or -forbidden modes. Water gives rise to strong IR bands including the stretching and bending modes at

ca. 3400 and 1630 cm^{-1}, respectively. The bending mode represents a major difficulty in studying biological samples due to overlapping with the amide I band in the spectra of proteins (see below). In IR transmission measurements, therefore, cuvettes of very small optical paths (a few micrometers) and very high protein concentrations have to be employed. The attenuated total reflection (ATR) technique allows bypassing the problems associated with water, facilitating the studies of protein/substrate or protein/ligand interactions, and enhancing the overall sensitivity. In Raman spectroscopy water is not an obstacle at room temperature, although ice lattice modes become visible in the low frequency region in croygenic measurements. A severe drawback of Raman spectroscopy is its low sensitivity, due to the low quantum yield of the scattering process ($< 10^{-9}$). This disadvantage can be overcome for molecules that possess chromophoric cofactors, such as metalloproteins. When the energy of the incident laser light is in resonance with an electronic transition of the chromophore, the quantum yield of the scattering process becomes several orders of magnitude higher for the vibrational modes originating from the chromophore. Thus, the sensitivity and the selectivity of Raman spectroscopy (i.e., resonance Raman – RR) are strongly increased and the resultant spectra display only the vibrational modes of the cofactor, regardless of the size of the protein matrix (Siebert and Hildebrandt, 2008).

In the last decades RR spectroscopy was proved to be indispensable in the studies of heme proteins. RR spectra obtained upon excitation into the Soret band of the porphyrin display ´so-called´ core-size marker bands sensitive to the redox and spin state and coordination pattern of the heme iron in the 1300 – 1700 cm^{-1} region (Hu *et al.*, 1993; Spiro and Czernuszewicz, 1995; Siebert and Hildebrandt, 2008). For instance, transition from a ferric to a ferrous heme is associated with a ca. 10 cm^{-1} downshift of most of the marker bands (particularly ν_3 and ν_4). The conversion from a six-coordinated low spin (6cLS) heme to a five-cordinated high spin (5cHS) heme also causes a downshift of some bands (ν_3 and ν_2). These and further empirical relationships derived from a large experimental data basis provide valuable tools for elucidating structural details of the heme site and for monitoring ET and enzymatic processes, as shown for a variety of heme proteins including hemoglobin, myoglobin, cytochromes, peroxidases and oxygen reductases (Spiro and Czernuszewicz, 1995; Siebert and Hildebrandt, 2008).

IR spectra provide information on the secondary structure of proteins based on the analysis of the amide I (1600 – 1700 cm^{-1}) and amide II (1480 – 1580 cm^{-1}) bands. The sensitivity and selectivity of IR spectroscopy can be greatly improved upon operating in difference mode. Difference IR spectra obtained from two states of a protein only display those bands that undergo a change upon transition from one state to the other, thereby substantially simplifying the analysis (Ataka and Heberle, 2007). IR difference spectroscopy is a sensitive method for investigating structural changes of proteins that (i) accompany the redox reaction, (ii) are induced by substrate binding during the catalytic cycle, (iii) occur during protein folding and unfolding, or (iv) accompany photo-induced processes (Siebert and Hildebrandt, 2008).

4.2 Surface Enhanced resonance Raman (SERR) and surface enhanced IR (SEIRA) spectroscopy

Surface enhanced Raman (SER) spectroscopy is based on the increase of the signal intensity associated with vibrational transitions of molecules situated in close proximity to nanoscopic metal structures. Two distinct enhancement mechanisms have been identified. The chemical mechanism originates from charge transfer interactions between the metal substrate and the adsorbate, and provides a weak enhancement solely for the molecules in direct contact with the metal. The electromagnetic mechanism is based on the amplified electromagnetic fields generated upon excitation of the localized surface plasmons of nanostructured metals. It does not require specific substrate/adsorbate contacts and provides the main contribution to the overall enhancement. Among different metals tested as SER substrates, Ag affords the strongest electromagnetic enhancements, due to surface plasmon resonance in a wide spectral range from the near UV to the IR region. A drawback, however, is that Ag nanostructures are less stable and chemically less inert than their Au counterparts. In addition, the low oxidation potential of Ag narrows the range of applicable potentials in SER-based spectro-electrochemical experiments. For these reasons most efforts in recent years have been devoted to the development of Au SER substrates, including SER-active electrodes. The attractiveness of the unsurpassed sensitivity of Ag has also driven significant efforts towards use of this metal and hybrid Ag/Au structures. To this end, a large number of highly regular and reproducible Au and Ag SER substrates have been reported, making use of spheres, tubes, rods, thorns, cavities and wires as building blocks (Mahajan *et al.*, 2007; Murgida and Hildebrandt, 2008; Lal *et al.*, 2008; Banholzer *et al.*, 2008; Brown and Milton, 2008; Feng *et al.*, 2008a; Feng *et al.*, 2009).

If the excitation laser is in resonance not only with the energy of surface plasmons of the metal but also with the electronic transition of the immobilized molecule, the SER and RR effects combine. The resulting SERR spectra display exclusively the vibrational bands of the chromophore of the adsorbed species. The use of Ag as SER-active substrate is particularly suited for studying porphyrins and heme proteins since these molecules exhibit a strong electronic transition at ca. 410 nm (Soret band) and a weaker one at ca. 550 nm which both coincide with Ag (but not with Au) surface plasmon resonances. SERR spectra of heme proteins reveal the same information as RR spectra, such as the oxidation, spin, and coordination states of the heme group, and in addition their changes as a consequence of variations of the electrode potential (see bellow) (Siebert and Hildebrandt, 2008).

Molecules adsorbed in the vicinity of nanostructured metal surfaces, such as Ag or Au islands deposited on inert ATR crystals, experience enhanced absorption of IR radiation, which is the basis for (ATR) SEIRA spectroscopy. SEIRA spectroscopy has been successfully employed to probe the structure of immobilized biomolecules including redox proteins and enzymes (Ataka and Heberle, 2007). The enhancement of the IR bands does not exceed two orders of magnitude and therefore is smaller than the enhancement of the SERR bands which may be larger than 10^5. The distance-dependent decay of the enhancement factor is less pronounced for SEIRA than for SERR spectroscopy, and both techniques can successfully probe molecules separated from the surface by up to 5 nm.

The nanostructured metal substrate that amplifies the signals can also serve as a working electrode in spectroelectrochemical studies. Indeed, potentiometric titrations followed by SERR and SEIRA have provided important insights into the mechanism of functioning of

several heme proteins immobilized on biocompatible metal electrodes (Murgida and Hildebrandt, 2004a; Murgida and Hildebrandt, 2005; Murgida and Hildebrandt, 2008).

Both SERR and SEIRA can be employed in the time resolved (TR) mode that enables probing of dynamics of immobilized proteins. The method requires a synchronization of a perturbation event with the spectroscopic detection at variable delay times. For TR-SEIRA spectroscopy acquisition is usually performed in the rapid or step scan mode for probing events in time windows longer or shorter than 10 ms, respectively. For the study of potential dependent processes of immobilized redox proteins by TR-SERR, the equilibrium of the immobilized species is perturbed by a rapid potential jump, and the subsequent relaxation process is then monitored at different delay times. A prerequisite for applying of TR-SERR is that the underlying ET processes are fully reversible. The time resolution depends on the charge reorganization of the double layer of the working electrode and is typically on a microsecond scale (Murgida and Hildebrandt, 2004a; Murgida and Hildebrandt, 2005; Murgida and Hildebrandt 2008).

5. Recent developments in the characterization of immobilized redox proteins

In this section we will focus on selected examples of surface enhanced spectroelectrochemical characterization of ET proteins immobilized on nanostructured electrodes coated with biomimetic films. The first part is dedicated to membrane oxygen reductases whose structural, functional and spectroscopic complexity imposes some serious limits to other experimental approaches. In the second part we will describe recent studies on soluble electron carrier proteins, mainly cytochromes.

5.1 Membrane proteins: oxygen reductases
Terminal oxygen reductases are the final complexes in aerobic respiratory chains that couple the four-electron reduction of molecular oxygen to water with proton translocation across the membrane (vide supra). Intense research efforts have been made in the past decades to elucidate the mechanism of the molecular functioning of these enzymes. Although substantial progress has been made, for instance, in determining their three-dimensional structures, the coupling between the redox processes and proton translocation is not yet well understood (Garcia-Horsman et al., 1994; Pereira and Teixeira, 2004). Most of the terminal oxidases are members of the heme - copper superfamily that can be classified into several families, based on amino acid sequences and intraprotein proton channels. The members of the family A are mitochondrial–like, possessing amino acid residues that compose D and K channels, the B-type enzymes have an alternative K channel, while members of the C family possess only a part of the alternative K channel. Oxygen reductases from bacteria and archaea reveal different subunit and heme-type compositions (Figure 4); they are simpler than the eukaryotic ones while maintaining the same functionality and efficiency. The mitochondrial Cyt-c oxidase (CcO) possesses 13 subunits, while the bacterial heme - copper oxidases, that are also efficient and functional proton pumps, contain three to four (Gennis, 1989; Garcia-Horsman et al., 1994; Pereira and Teixeira, 2004). Investigating the catalytic reaction of bacterial complexes is therefore fundamental as the obtained insights can be extrapolated to the eukaryotic ones. A prerequisite for understanding the mechanism of functioning of these enzymes that contain multiple redox centers is determination of the individual midpoint redox potentials of the cofactors under conditions that reproduce some

basic features of the physiological environment. Published redox properties of oxygen reductases are typically determined from solution studies and are often contradictory regarding both the values and the interpretation (Todorovic *et al.*, 2005; Veríssimo *et al.*, 2007). In this respect, the use of SERR spectroelectrochemical titrations has been proven to be a valuable tool.
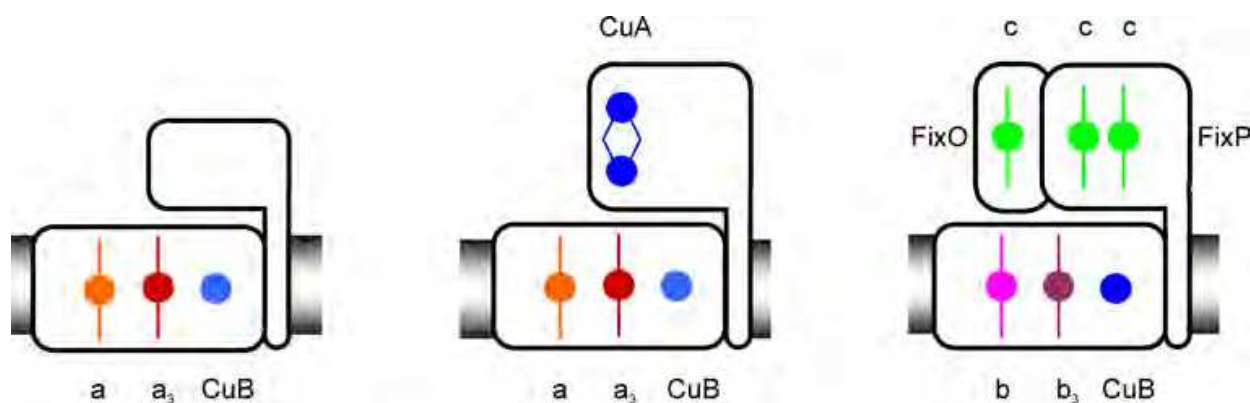

Fig. 4. Schematic representation of several oxygen reductases. A) *aa₃* quinol oxidase; B) *aa₃* cytochrome c oxidase; C) *cbb₃* oxygen reductase. The LS hemes in the respective catalytic subunits are depicted in orange (heme *a*) and pink (heme *b*), the HS hemes are in red (*a₃*) and purple (*b₃*), the LS hemes *c* in FixO and FixP subunits of the *cbb₃* are shown in green, and copper centers (dinuclear Cu_A and Cu_B), in blue.

aa₃ quinol oxidase (QO): The *aa₃* oxygen reductase from the thermophylic archaeon *Acidianus ambivalens* receives electrons directly from the membrane quinone pool, being therefore a quinol oxidase. It is a type B oxygen reductase that in the catalytic subunit houses two heme groups, the low-spin (LS) heme *a*, and the high spin (HS) heme *a₃* coupled to Cu_B in the catalytic (oxygen binding) center (Figure 4A). The two hemes display different RR spectral fingerprints. Detergent solubilized QO was directly adsorbed on a bare nanostructured Ag electrode and investigated by potential-dependent SERR (Todorovic *et al.*, 2005). Adsorption of the protein to the hydrophilic surface of the phosphate-coated electrode occurred without displacement of the detergent molecules, which therefore provided a biocompatible interface. This conclusion was supported by the detection of a SER signal at 2950 cm⁻¹ from the Ag electrode immersed into the protein-free buffer solution, that was attributed to the C-H stretching mode of dodecyl-maltoside. The protein retained its native structure upon immobilization as confirmed by the comparison of the RR and SERR spectra of QO in solution and in the adsorbed state (Figure 5A). Namely, all vibrational bands present in the RR spectra that were assigned to skeletal vibrations and stretching modes of the vinyl and formyl substituents of hemes *a* and *a₃* were identified in the SERR spectra of the immobilized QO. Variations of the band intensities between the SERR and RR spectra originate from the orientation-dependence of the SERR effect, which causes different enhancements of vibrational modes of HS vs. LS hemes, but also of modes of the same heme that have different symmetry (see 5.2). The spectra of immobilized QO, measured at a series of electrode potentials, were subsequently subjected to component analysis. At intermediate potentials, over forty modes could be identified in the high frequency region of the spectra, originating from the two heme groups in two redox states. In order to simplify the analysis and to avoid uncertainties caused by the overlapping of some modes, the quantitative

spectral analysis was based on two modes, the v_3 and $v_{C=O}$ that are unambiguous indicators of the redox and spin states of the two hemes. Simplified component spectra, based only on these modes of each heme group in each redox state, were constructed and used in a global fit to all experimental SERR spectra by varying the relative contributions of the individual component spectra (Figure 5B). After conversion of spectral contributions into relative concentrations, the redox potentials of the two heme sites in QO were determined. The corresponding Nernst plots display a linear behavior that reveals one-electron transfer processes, indicating, furthermore that the two hemes can be treated as independent redox couples with no significant interaction potential.

The results of the study point to a substantially different mechanistic scheme for the energy transduction in QO. The two redox centers, hemes *a* and *a*₃ are uncoupled and exhibit reversed midpoint potentials with respect to the type A enzymes. In both cases the free energy, provided by downhill ET reactions, is utilized for vectorial proton transport. However, for the type A enzymes the exergonicity of the ET cascade requires a sophisticated network of cooperativities. In contrast, downhill ET in QO is already guaranteed by the inversion of the intrinsic midpoint potentials of hemes *a* and *a*₃ such that a modulation by cooperativity effects is not required. Moreover, SERR experiments indicate that redox-linked, electric-field-modulated conformational transitions of the heme *a*₃ that are relevant for proton translocation, were blocked in the immobilized, but not in solubilized QO (Das *et al.*, 1999), suggesting furthermore that, when the membrane potential generated by the proton pumping activity of QO becomes sufficiently large, the resultant electric field is capable of blocking the elementary steps of proton translocation. This finding has been interpreted in terms of a self-regulation mechanism of the proton pumping activity of the QO (Todorovic *et al.*, 2005).
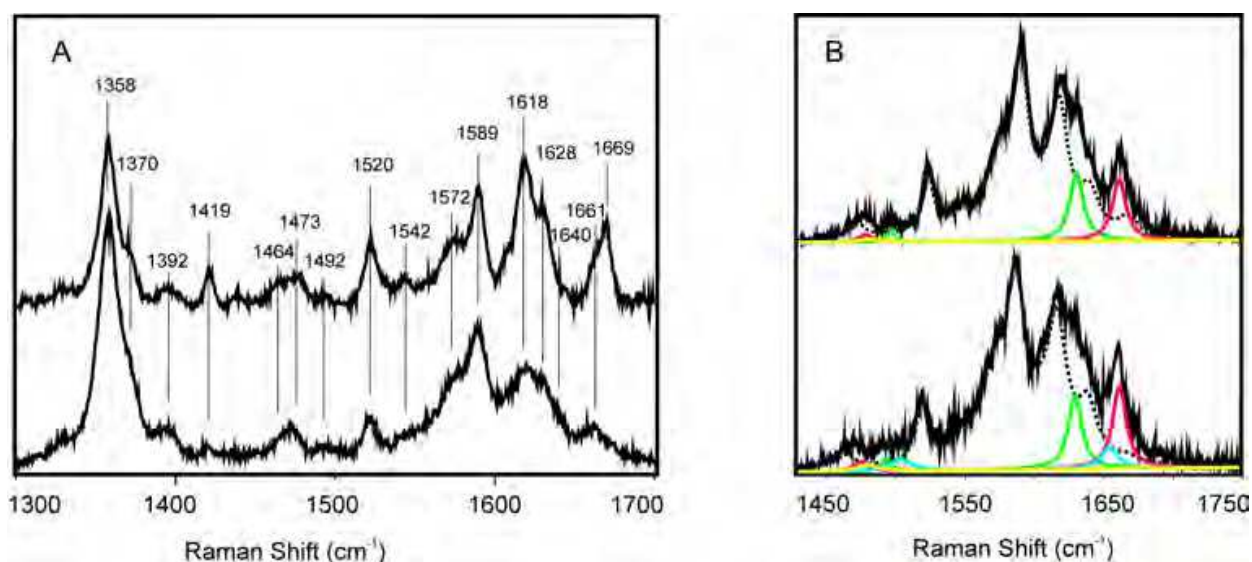

Fig. 5. RR and SERR spectra of the *aa*₃ QO. A) high frequency region spectra of reduced QO: RR of solubilized (upper trace) and SERR of immobilized (lower trace) protein; B) SERR spectra of the QO at - 3 mV (upper trace) and at + 297 mV (lower trace). Vibrational modes of the heme *a* are indicated in green (ferrous) and blue (ferric); modes of the heme *a*₃ are shown in red (ferrous) and yellow (ferric); dotted line represents the envelope that includes all non-assigned bands, black line shows experimental and overall simulated spectra.

aa₃ cytochrome c oxidase: The CcO from *Rhodobacter sphaeroides* is a member of the type A family of heme copper oxygen reductases that houses three redox centers in the catalytic subunit (subunit I) and a dinuclear copper Cu$_A$ in the subunit II (Figure 4B). It is purified from an organism that is capable of growing heterotrophically via fermentation and aerobic and anaerobic respiration, with a genetically introduced His-tag, allowing immobilization of the CcO on a metal electrode via Ni-NTA SAMs, Figure 3C (Friedrich *et al.*, 2004; Ataka *et al.*, 2004; Giess *et al.*, 2004; Hrabakova *et al.*, 2006; Todorovic *et al.*, 2008). The protein was specifically attached, uniformly oriented and catalytically active in the biomimetic construct. The orientation of the attached protein could be controlled since the His-tag was introduced into the amino acid sequence of *R. sphaeroides* enzyme either on the C-terminus of subunit I or on the C-terminus of subunit II. Therefore, the domain that interacts with the physiological electron donor, Cyt-c, identified to be composed of residues Glu148, Glu157, Asp195, and Asp214 in subunit II, was either exposed to the solution, or was facing the metal surface (Ataka *et al.*, 2004). Catalytic currents could be measured under aerobic conditions when the Cyt-c / CcO complex was allowed to form. Proton pumping activity was also functional in the construct, as suggested by electrochemical impedance spectroscopy. SERR spectroscopic studies revealed heterogeneous ET to the heme *a*, which was selectively reduced while the heme *a₃* remained oxidized, even at the most negative electrode potentials. The ET between the two hemes is fast in solution, indicating some alterations of the intramolecular ET in immobilized CcO, possibly due to electric field dependent perturbation of internal proton translocation steps (Hrabakova *et al.*, 2006).

cbb₃ oxygen reductase: The *Bradyrhizobium japonicum cbb₃* oxidase is a type C oxygen reductase that contains three major subunits: a membrane integral subunit I (FixN), which houses a LS heme *b* and the catalytic center (HS heme *b₃* - Cu$_B$), and subunits II (FixO) and III (FixP), containing one (His-Met coordinated) and two (bis His and His-Met coordinated) LS hemes *c*, respectively (Figure 4C). The *cbb₃* oxygen reductases are expressed in various bacteria under microaerobic conditions and exhibit several unique characteristics (Sharma *et al.*, 2006). Phylogenetically, they are the most distant and the least understood members of the heme-copper oxygen reductase superfamily (Pereira and Teixeira, 2004; Pitcher and Watmough, 2004; Sharma *et al.*, 2006). The *cbb₃* oxygen reductases lack the Cu$_A$ electron entry site (Garcia-Horsman *et al.*, 1994) and the highly conserved tyrosine residue covalently bound to the histidyl Cu$_B$ ligand. Furthermore, many of the amino acid residues involved in proton conduction through the D- and K- channels of the A-type enzymes are absent in *cbb₃* oxygen reductases. These enzymes exhibit the highest NO reductase activity among the members of the superfamily (Forte *et al.*, 2001; Pitcher and Watmough, 2004; Veríssimo *et al.*, 2007). The *cbb₃* oxygen reductase from *B. japonicum* possesses a genetically introduced His tag on the C-terminus of subunit I, i.e. on the cytoplasmic side. As in the previous example, it was immobilized on Ag (and Au) electrode coated with a (Ni-NTA) SAM, embedded into a reconstituted phospholipid bilayer, Figure 3C, and studied by surface-enhanced vibrational spectroscopy and cyclic voltammetry (Figure 6) (Todorovic *et al.*, 2008).
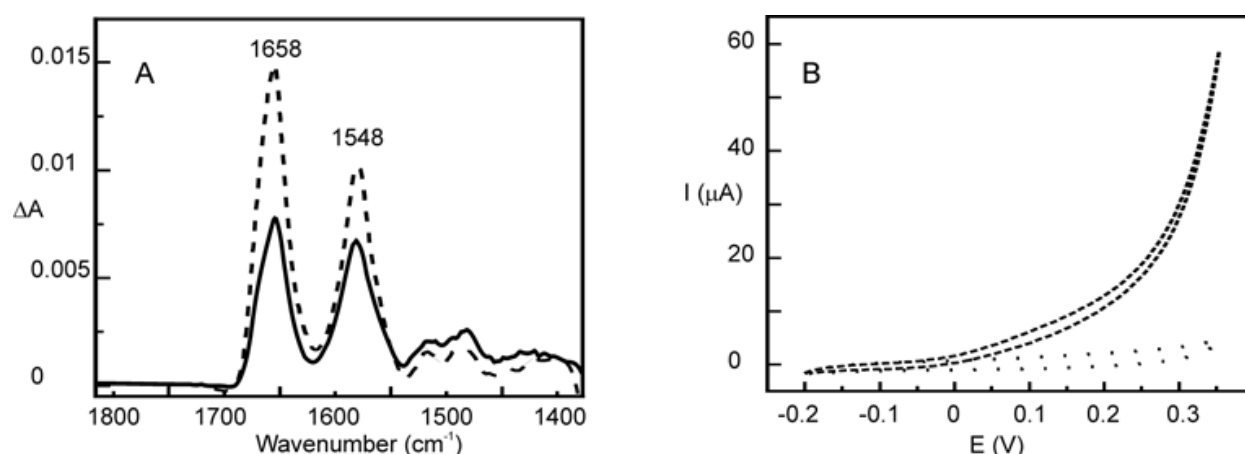
Fig. 6. Immobilized cbb_3 oxygen reductase. A) SEIRA spectra of the cbb_3 immobilized via His-tag/Ni-NTA (dashed line) and detergent coated electrode (solid line); B) cyclic voltammetry of the cbb_3 embedded into biomimetic construct in the presence (dashed line) and absence (dotted line) of electron donor.

SEIRA spectra of the immobilized cbb_3 are dominated by the amide I and II modes (Figure 6A). For membrane proteins with a high content of preferentially parallel helices such as the subunit I of cbb_3 (Zufferey *et al.*, 1998; Pitcher and Watmough, 2004), SEIRA spectra are sensitive to the orientation of the helices with respect to the electrode surface, which is reflected in the intensity ratio of amide I and amide II bands. The amide I mode, that is mainly composed by the C=O stretching coordinates of the peptide bonds, is associated with dipole moment changes parallel to the axis of the helices, such that it gains surface enhancement when the C=O groups, and thus the helices, are oriented perpendicular to the surface. Conversely, the dipole moment changes of the amide II mode that is mainly composed of N-H in-plane bending and C-N stretching coordinates, are perpendicular to the helix axis and therefore gain a weaker enhancement for helices oriented in an upright position (Marsh *et al.*, 2000). In the SEIRA spectrum of cbb_3 the amide I is observed at 1658 cm^{-1}, a characteristic position for a largely α-helical peptide. Its intensity is distinctly higher than that of the amide II (1548 cm^{-1}), which is consistent with a largely perpendicular orientation of the helices with respect to the electrode surface. A more random orientation of the enzyme is obtained upon non-specific adsorption of the solubilized cbb_3 on a detergent-coated electrode as reflected by a ca. two times weaker amide I band and a 1.5 times lower amide I / amide II intensity ratio, compared with the His-tag bound cbb_3 (Figure 6A) (Todorovic *et al.*, 2008). The oxygen reductase catalytic activity of the immobilized cbb_3 was controlled *in situ* by cyclic voltammetry. As shown in Figure 6B, large electrocatalytic currents are observed under aerobic conditions in the presence of the electron donor, while only capacitive currents were observed in its absence.

Unlike the aa_3 QO and CcO, the cbb_3 oxygen reductase possesses five heme groups, three of which are 6cLS c-type hemes that are spectroscopically indistinguishable. Moreover, four out of five hemes are LS, displaying higher Raman cross sections, and therefore partially obscuring the spectroscopic features of catalytic HS heme b_3. Reliable component analysis of the SERR spectra was further aggravated by the high photoreducibility of the enzyme. Therefore, in order to facilitate the assignment of individual redox transitions to each heme group of the pentahemic cbb_3, the individual FixO and FixP subunits (Figure 4C) were

overexpressed in *E. coli* with their transmembrane domain truncated, purified in soluble form, and characterized by SERR spectroelectrochemistry. Upon combining the SERR-spectroelectrochemical data for the subunits and for the integral enzyme, it was possible to provide a consistent analysis of redox potentials of the individual cofactors in the *cbb*$_3$ oxidase. On the basis of these findings, a sequence of ET events in the *cbb*$_3$ enzyme was postulated. The Met/His heme *c* of either the FixO or FixP subunit, which exhibit the lowest redox potentials, serves as the electron entry site of the complex. According to the order of redox potentials, the subsequent electron acceptor was identified as the bis-His heme *c* in the FixP or/and the HS heme *b* in the catalytic subunit, and the final one is the heme *b*$_3$ (Todorovic, *et al.*, 2008). The obtained data also shed light on a controversially discussed role of the FixP subunit in *cbb*$_3$ oxygen reductases. The values of redox potentials obtained by SERR potentiometric titration reveal that the presence of FixP can be considered as redundant in the ET pathway. Rather, it can be associated with oxygen sensing properties, as also suggested for the *cbb*$_3$ enzyme from *P. stutzeri* (Pitcher and Watmough, 2004b).

5.2 Soluble proteins

As discussed in previous sections, small soluble redox proteins that transport electrons between different membrane-bound complexes along biological ET chains are exposed to relatively intense electric fields which may have a substantial impact on their structure and function. Among these electron shuttles, cytochromes and particularly Cyt-c, constitute the best studied examples. Electric field effects on the structure, thermodynamics and reaction dynamics of cytochromes have been extensively investigated using Ag electrodes coated with SAMs of ω-substituted alkanethiols as biomimetic interfaces that allow a systematic variation of the field strength (see 3.2).

Electric field effects on redox potential. Among other parameters, electric fields of biologically relevant magnitude may affect the most fundamental thermodynamic property of a redox protein, i.e. its reduction potential. This has been shown by potential-dependent SERR spectroscopy for the soluble tetraheme protein cytochrome *c*$_3$ (Cyt-c$_3$) (Rivas *et al.*, 2005). Electrostatic adsorption of Cyt-c$_3$ on Ag electrodes coated with mercaptoundecanoic acid occurs without significant structural alterations at the level of the heme groups. SERR potentiometric titrations, however, indicate that the redox potentials of the four hemes are significantly downshifted with respect to their values in solution, to such an extent that the order of reduction is actually reversed. The experimental results, that were in excellent agreement with electrostatic calculations, revealed that electric fields tend to downshift the redox potentials by stabilizing the ferric form. This effect is partially compensated by the low dielectric constant of the SAM which shifts the redox potentials in the opposite direction. Indeed, the resulting downshift was more pronounced for the hemes that are closer to the interface, i.e. under the influence of higher electric fields.

A similar interplay of different effects on the redox potential has been observed for cytochrome P450 from *P. putida* immobilized on coated Ag electrodes, although in this case the adsorbed protein was almost quantitatively converted into the P420 form as judged from the SERR spectra (Todorovic *et al.*, 2006). In contrast, electrostatic adsorption of Cyt-c on similar coatings does not appear to have any significant effect on the redox potential but may have distinct structural implications (Murgida and Hildebrandt, 2001a; Murgida and Hildebrandt, 2004a).

Electric field effects on protein structure and function. It has been established, using RR and SERR spectroscopy, that the electrostatic interaction of the positively charged Cyt-c with negatively charged model systems, such as phospholipid vesicles, (Droghetti *et al.*, 2006), polyelectrolytes (Weidinger *et al.*, 2006), or the binding domain of the natural reaction partner CcO, may promote the formation of the conformational state of mitochondrial Cyt-c (denoted as B2), in which the axial Met80 ligand is removed from the heme iron. At physiological pH, this coordination site may remain vacant, resulting in 5cHS Cyt-c, or may be occupied by a His residue (most likely His26 or His33). The disruption of the Fe-Met80 bond significantly alters the properties of Cyt-c. On the one hand, the B2 state has a reduction potential which is more than 300 mV lower than that of the native protein (denoted as state B1) as determined by potential-dependent SERR spectroscopy (Murgida and Hildebrandt, 2004a). On the other hand, the B2 state shows a substantial increase of peroxidase activity by allowing the access for hydrogen peroxide to the heme iron (Kagan *et al.*, 2005; Godoy *et al.*, 2009). Thus, *in vivo* the B1 to B2 transition would have profound physiological consequences since the B2 state cannot accept electrons from complex III but is capable of catalyzing the peroxidation of cardiolipin, the main charged lipid component of the inner mitochondrial membrane (Kagan *et al.*, 2009). Degradation of cardiolipin increases the permeability of the membrane, thus facilitating the transfer of Cyt-c to the cytosol where it binds to Apaf-1, in one of the initial events of the cell apoptosis. Thus, it is likely that the switch from the "normal" redox function of Cyt-c (B1 state) to the apoptotic function (B2 state) depends on the local electric field which is, in turn, modulated by the membrane potential. To check this hypothesis the structure of Cyt-c electrostatically bound to electrodes coated with anionic SAMs was investigated. Variation of the electrode potential and of the charge density on the film surface shows that the equilibrium between the B1 and B2 states of the protein is shifted towards B2 upon raising the electric field strength at the interface of the biomimetic construct (Murgida and Hildebrandt, 2001a; Murgida and Hildebrandt, 2004a). Detailed spectroscopic studies, including a variety of techniques, have demonstrated that the B1 to B2 transition occurs without substantial alteration of the protein secondary structure. Based on these observations, the influence of the electric field on the dissociation energy of the Fe-Met80 bond in model porphyrins were studied using density functional theory (DFT). In that case, i.e., for the isolated heme moiety lacking the protein environment, no significant effect on the Fe-S(Met) bond stability was predicted for biologically meaningful electric field strengths (De Biase *et al.*, 2007). On the other hand, molecular dynamics simulations performed on the entire protein, show that biologically relevant electric fields induce an increased mobility of the key protein segments that lead to the detachment of the sixth axial ligand, Met80, from the heme iron. This electric-field induced conformational transition is both energetically and entropically driven (De Biase *et al.*, 2009). It was proposed, based on these theoretical and experimental investigations using biomimetic systems, that the variable transmembrane potential may modulate the structure of Cyt-c, thus playing the role of a switch that can alternate its redox function in the respiratory chain to peroxidase function in the early events of apoptosis.

Electric field effects on protein dynamics. Protein dynamics has been recently recognized as a key factor in controlling or limiting inter- and intra-protein ET reactions. However, in most of the cases the complexity of biological systems impairs direct observations of processes such as conformational gating, configurational fluctuations or rearrangement of protein complexes under reactive conditions. In this context simplified model systems, like proteins

immobilized on SAM-coated electrodes, can greatly contribute to the understanding of the biophysical fundamentals in better detail, even though they unavoidably deviate from the true physiological conditions. A specific advantage of this approach is facilitating the determination of ET rate constants as a function of distance by simply varying the chain length of the alkanethiols without modifying other experimental parameters (Murgida and Hildebrandt, 2001a; Murgida and Hildebrandt, 2001b). For redox proteins immobilized on SAM-coated metal electrodes one can anticipate a nonadiabatic ET mechanism. Therefore, the kinetics of the heterogeneous ET reaction can be described according to the high temperature limit of Marcus semiclassical expression, including integration to account for all the electronic levels of the metal, ε, contributing to the process (Marcus, 1965):

$$k_{ET} = \frac{\pi}{\hbar} \frac{|V|^2 \rho}{\sqrt{\pi \lambda k_B T}} \int_{-\infty}^{\infty} \exp\left[-\left(\frac{\left(\lambda + (\varepsilon_F - \varepsilon) + e\eta^0\right)^2}{4\lambda k_B T}\right)\right] \frac{1}{1 + \exp\left[(\varepsilon - \varepsilon_F)/k_B T\right]} d\varepsilon \qquad (2)$$

where $\rho(\varepsilon)$, $f(\varepsilon)$, $|V|$, ε_F, and λ are the density of electronic states in the electrode, the Fermi-Dirac distribution, the magnitude of the electronic coupling, the energy of the Fermi level, and the reorganization energy of the redox active molecule. The quantity $\eta^0 = (E - E^0)$ refers to the standard overpotential, with E denoting the actual electrode potential and E^0 the standard potential for the redox couple; the other parameters in Equation 2 have the usual meaning. The electronic coupling decays exponentially with the distance separating the redox center from the electrode.

Notably, the characteristic exponential decay of k_{ET} with the distance predicted by the theory is verified only partially in most studies reported so far. Indeed, several research groups have studied the distance-dependence of the ET rates for a variety of proteins immobilized on Au and Ag electrodes coated with pure and mixed SAMs of ω-functionalized alkanethiols using TR-SERR and electrochemistry. These studies include Cyt-c immobilized on COOH-, COOH/OH, CH$_3$-, and pyridine-terminated SAMs, (Murgida and Hildebrandt, 2001a; Murgida and Hildebrandt, 2002; Yue et al., 2006; Murgida et al., 2004b; Feng et al., 2008b) cytochrome b_{562} on NH$_2$-terminated SAMs (Zuo et al., 2009), azurin on CH$_3$-terminated SAMs (Murgida et al., 2001a) and cytochrome c_6 (Kranich et al., 2009) and Cu$_A$ (Fujita et al., 2004) centers on mixed SAMs, among others. In all the cases, the measured ET rates verify the expected exponential decay with distance, but only for relatively thick SAMs. For thinner SAMs, however, the measured rate was distance-independent even though, due to the still long donor-acceptor separation (> 6 Å), a non-adiabatic ET mechanism should apply (Figure 7A). The origin of this behavior has been elusive and controversial for the last ten years.

Recently, the use of SER selection rules for analyzing the reaction dynamics of immobilized heme proteins has shed some light onto this issue (Kranich et al., 2008). In a SER experiment, i.e. under off-resonance conditions, the individual components of the scattering tensor of the heme are modified depending on the direction of the electric field vector and the orientation of the heme plane. Assuming an ideal D_{4h} porphyrin symmetry, one can anticipate that the A_{1g} modes will experience preferential enhancement when the heme plane is parallel to the surface, while for a perpendicular orientation A_{1g}, A_{2g}, B_{1g} and B_{2g} will all be enhanced. Therefore, different orientations of the adsorbed heme protein are expected to lead to different intensity ratios of modes of different symmetries, e.g. $\nu_{10}(B_{1g})/\nu_4(A_{1g})$. These SER

selection rules do not hold when the experiments are performed under electronic resonance conditions (SERR), i.e. Soret excitation, typically used in the studies of heme proteins.
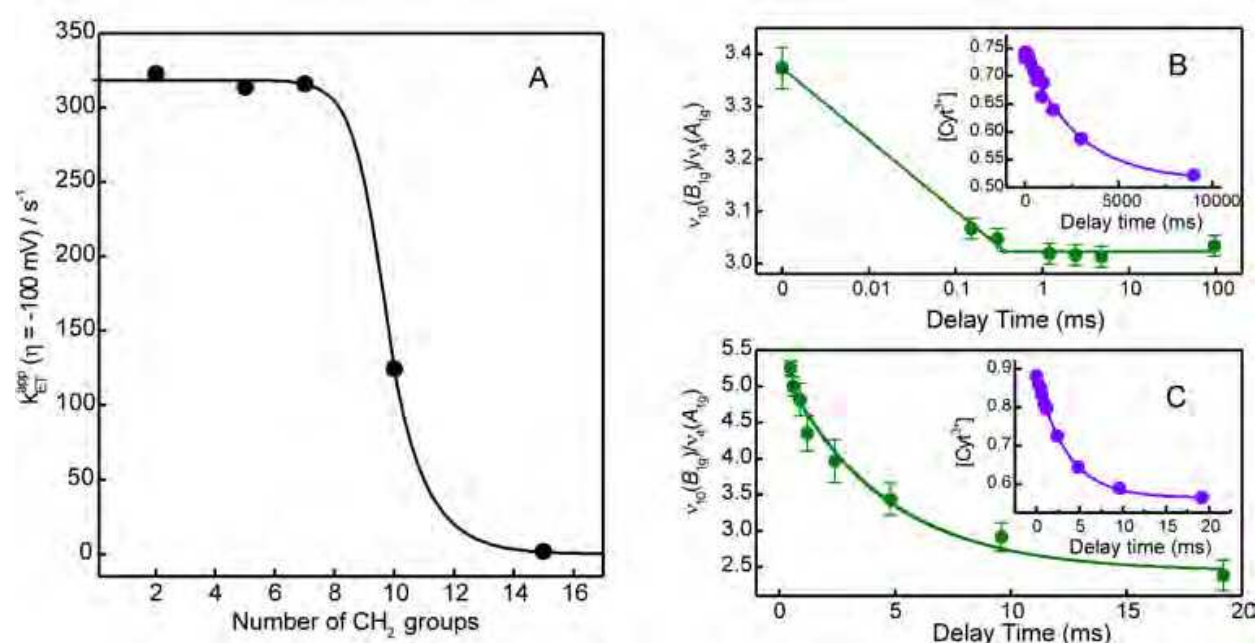

Fig. 7. TR-SERR data of Cyt-c electrostatically adsorbed to COOH-terminated SAMs. A) distance-dependence of the apparent ET rates determined at η = -100 mV; B) time-dependence of the v_{10}/v_4 intensity ratio (green, λ_{exc} = 514 nm) and of the concentration of ferric protein (violet, λ_{exc} = 413 nm) for Cyt-c adsorbed on SAM with 15 CH_2 groups; C) idem (B) for a SAM with 5 CH_2 groups.

In that case SERR spectra are largely dominated by the totally symmetric modes A_{1g}, which, in addition to partial scrambling of the radiation, result in an almost complete loss of orientation information. However, a reasonable compromise between acceptable enhancement and qualitatively predictable selection rules can still be achieved upon excitation into the less intense Q electronic transition of heme, by which non-totally symmetric modes are also enhanced.

This strategy has been applied for investigating the reaction dynamics of Cyt-c and Cyt-c$_6$ electrostatically adsorbed on Ag electrodes coated with SAMs of ω-carboxyl alkanethiols. TR-SERR experiments performed under Q-band excitation show that, upon applying a potential jump, the protein reorients within the electrostatic complex. The reorientation is fast in the low electric field regime, i.e. long SAMs, but becomes slower at shorter SAMs due to the barrier imposed by the increasing electric field. Indeed it has been observed that the measured ET rates in the plateau region of the k_{ET} vs. distance plots are identical to the reorientation rates, implying that reorientation is the rate limiting step (Figure 7). To understand these results at a molecular level, molecular dynamics simulations of the biomimetic systems were performed (Paggi *et al.*, 2009). The simulations show that Cyt-c can adsorb on SAMs in a variety of orientations that imply two major binding sites situated around the partially exposed heme group. In the low electric field regime, the electrostatic complexes are characterized by a large mobility of the protein that leads to significant fluctuations of the electronic coupling ($|V|$ in equation 2). For examples, a 7° change of tilt

angle of the heme with respect to the electrode plane may change the ET rate constant by more than two orders of magnitude. Moreover, the protein mobility is significantly restricted upon increasing the interfacial electric field. Thus, TR-SERR studies of heme proteins in biomimetic devices suggest that the initial electrostatic complex is not necessarily optimized for ET in terms of electronic pathway efficiency. Therefore, for the ET reaction to take place, the protein needs to reorient in search for higher electronic couplings. While at low interfacial electric fields and long tunneling distances this process is comparatively fast, it may become rate limiting at higher field strengths.

Electric field control of ET rates via modulation of protein dynamics seems to be a widespread phenomenon in bioelectrochemistry and protein-based bioelectronics. One can envisage similar effects controlling inter-protein ET *in vivo*, for example in photosynthetic and respiratory chains. In fact, the results obtained with the biomimetic systems are consistent with the biphasic kinetics observed for the inter-protein ET reactions between Cyt-c and CcO, on one hand, and between Cyt-c$_6$ and photosystem I, on the other (Murgida and Hildebrandt, 2008). In both cases, the cascade of ET reactions is coupled to proton translocation across the membrane generating a gradient that drives the ATP synthesis. This implies variable electric field strength during turnover, affecting the sampling rate of optimal ET pathways in transient and long-lived complexes between membrane bound proteins and soluble electron carriers. Such an effect might constitute the basis for a feedback regulating mechanism (Murgida and Hildebrandt, 2008).

6. Conclusions and Outlook

Within the past two decades, enormous progress has been achieved in developing tailored strategies for immobilizing proteins on functionalized metal surfaces. These achievements are reflected by the increasing number of biotechnological applications of enzyme-based bioelectronic devices. Yet, the behavior of the immobilized proteins is by far not understood, which aggravates employing rational design principles for the fabrication and optimization of bioelectronic devices. In this respect, surface-enhanced vibrational spectroscopies that have been introduced in this contribution are promising tools for elucidating structure and reaction dynamics of immobilized proteins. The examples presented in the previous section document the high potential of these techniques that are not only relevant for promoting the biotechnological development in this field but may also substantially improve the understanding of fundamental biophysical and biochemical processes in vivo. Nevertheless, both SERR and SEIRA spectroscopies are currently associated with some restrictions which narrow the range of applications. Specifically, these techniques require nanostructured Ag and Au surfaces as signal-amplifying media. These metals are usually not the type of solid supports used in biotechnological applications. Furthermore, the nanoscopic surface morphology might perturb the structure of membrane-like coatings, a drawback for using these devices as biomimetic systems for biological membranes. However, these limitations may be overcome in the near future taking into account recent promising developments in nanotechnology and material science such as the fabrication of bi-metallic hybrid systems, tailored metal nanoparticles, or surfaces with ordered nanoscopic morphologies.

7. References

Arya, SK, Solanki PR, Datta M, and Malhotra BD (2009) Recent advances in self-assembled monolayers based biomolecular electronic devices. *Biosens. Bioelectron.*, 24, 2810-2817.

Ataka K, Giess F, Knoll W, Naumann R, Haber-Pohlmeier S, Richter B, and Heberle J (2004) Oriented attachment and membrane reconstitution of his-tagged cytochrome c oxidase to a gold electrode: In situ monitoring by Surface-Enhanced Infrared Absorption spectroscopy. *J. Am. Chem. Soc.*, 126, 16199-16206.

Ataka K and Heberle J (2007) Biochemical applications of Surface-Enhanced Infrared Absorption spectroscopy. *Anal. Bioanal. Chem.*, 388, 47-54.

Banholzer MJ, Millstone JE, Qin L, and Mirkin CA (2008) Rationally designed nanostructures for surface-enhanced Raman spectroscopy. *Chem. Soc. Rev.* 37, 885-897.

Brown RJC and Milton MJT (2008) Nanostructures and nanostructured substrates for surface - enhanced Raman scattering (SERS). *J. Ram. Spec.*, 39, 1313-1326.

Cass T (2007) Enzymology, in Marks, RS, Cullen, DC, Karube, I, Lowe, CR, and Weetall, H H (Eds.), *Handbook of biosensors and biochips 1*. John Wiley & Sons Ltd, Chichester, 84-99.

Clarke JR (2001) The dipole potential of phospholipid membranes and methods for its detection. *Adv. Colloid. Interface Sci.* 89-90, 263-281.

Collier JH and Mrksich M (2006) Engineering a biospecific communication pathway between cells and electrodes. *Proc. Natl. Acad. Sci.*, 103, 2021-2025.

Das TK, Gomes CM, Teixeira M, and Rousseau DL (1999) Redox-linked transient deprotonation at the binuclear site in the *aa₃*-type quinol oxidase from *Acidianus ambivalens*: Immplications for proton translocation. *Proc. Natl. Acad. Sci.*, 96, 9591-9596.

De Biase PM, Doctorovich F, Murgida DH, and Estrin DA (2007) Electric field effects on the reactivity of heme model systems. *Chem. Phys. Lett.*, 434, 121-126.

De Biase PM, Paggi DA, Doctorovich F, Hildebrandt P, Estrin DA, Murgida D, and Marti MA (2009) Molecular basis for the electric field modulation of cytochrome *c* structure and function. *J. Am. Chem. Soc., in press*.

Droghetti E, Oellerich S, Hildebrandt P, and Smulevich G (2006) Heme coordination states of unfolded ferrous cytochrome c. *Biophys. J.*, 91, 3022-3031.

Feng JJ, Gernert U, Sezer M, Kuhlmann U, Murgida DH, David C, Richter M, Knorr A, Hildebrandt P, and Weidinger IM (2009) Novel Au-Ag hybrid device for electrochemical SE(R)R spectroscopy in a wide potential and spectral range. *Nano Lett.*, 9, 298-303.

Feng JJ, Hildebrandt P, and Murgida DH (2008a) Silver nanocoral structures on electrodes: A suitable platform for protein-based bioelectronic devices. *Langmuir*, 24, 1583-1586.

Feng JJ, Murgida D, Kuhlmann U, Utesch T, Mroginski MA, Hildebrandt P, and Weidinger I (2008b) Gated electron transfer of yeast iso-1 cytochrome c on self-assembled-monolayer-coated electrodes. *J. Phys. Chem. B*, 112, 15202-15211.

Forte E, Urbani M, Saraste M, Sarti P, Brunori M, and Giuffre A (2001) The cytochrome *cbb₃* from *Pseudomonas stutzeri* displays nitric reductase activity. *Eur. J. Biochem.*, 268, 6486-6491.

Friedrich MG, Gie F, Naumann R, Knoll W, Ataka K, Heberle J, Hrabakova J, Murgida D, and Hildebrandt P (2004) Active site structure and redox processes of cytochrome c oxidase immobilised in a novel biomimetic lipid membrane on an electrode. *Chem. Commun.*, 7, 2376-2377.

Fujita K, Nakamura N, Ohno H, Leigh BS, Niki K, Gray H, and Richards JH (2004) Mimicking protein-protein electron transfer: voltammetry of *Pseudomonas aeruginosa* azurin and the *Thermus thermophilus* Cu_A domain at omega-derivatized self-assembled-monolayer gold electrodes. *J. Am. Chem. Soc.*, 126, 13954-13961.

Garcia-Horsman JA, Barquera B, Rumbley J, Ma J, and Gennis RB (1994) The superfamily of the heme-copper respiratory oxidases. *J. Bacteriol.* 176, 5587-5600.

Gennis RB (1989). *Biomembranes: molecular structure and function.* Springer-Verlag, New York.

Giess F, Friedrich MG, Heberle J, Naumann R, and Knoll W (2004) The protein-tethered lipid bilayer: A novel mimic of the biological membrane. *Biophys. J.,* 87, 3213-3220.

Gilardi G (2004) Protein Engineering for Biosensors, in Cooper, J and Cass, AEG (Eds.), *Biosensors*, Oxford University Press, Oxford.

Godoy LC, Munoz-Pinedo C, Castro L, Cardaci S, Schonhoff CM, King M, Tortora V, Marin M, Miao Q, Jiang JF, Kapralov A, Jemmerson R, Silkstone GG, Patel JN, Evans JE, Wilson MT, Green DR, Kagan VE, Radi R, and Mannick JB (2009) Disruption of the M80-Fe ligation stimulates the translocation of cytochrome *c* to the cytoplasm and nucleus in nonapoptotic cells. *Proc. Natl. Acad. Sci.*, 106, 2653-2658.

Gupta R and Chaudhury NK (2007) Entrapment of biomolecules in sol-gel matrix for applications in biosensors: problems and future prospects. *Biosens. Bioelectron.*, 22, 2387-2399.

Haas AS, Pilloud KS, Reddy KS, Babcock GT, Moser CC, Blasie JK, and Dutton PL (2001) Cytochrome c and cytochrome c oxidase: Monolayer assemblies and catalysis. *J. Phys. Chem. B,* 105, 11351-11362.

Hasunuma T, Kuwabata S, Fukusaki E, and Kobayashi A (2004) Real-time quantification of methanol in plants using a hybrid alcohol oxidase-peroxidase biosensor. *Anal. Chem.*, 76, 1500-1506.

He JA, Samuelson L, Li J, Kumar J, and Tripathy SK (1999) Bacteriorhodopsin thin-film assemblies - immobilization, properties, and applications. *Adv. Mater.*, 11, 435-446.

Henning TP and Cunningham DD (1998) *Commercial Biosensors.* Wiley, New York, 3-46.

Hianik T (2008) Biological membranes and membrane mimics, in Bartlett, PN (Ed.) *Bioelectrochem.*, John Wiley and Sons, Chichester, 87-156.

Hodneland CD, Lee YS, Min DH, and Mrksich M (2002) Selective immobilization of proteins to self-assembled monolayers presenting active site-directed capture ligands. *Proc. Natl. Acad. Sci.*, 99, 5048-5052.

Hrabakova J, Ataka K, Heberle J, Hildebrandt P, and Murgida D (2006) Long distance electron transfer in cytochrome c oxidase immobilised on electrodes. A Surface Enhanced Resonanace Raman spectroscopic study. *Phys. Chem. Chem. Phys.*, 8, 759-766.

Hu S, Morris IK, Dingh JP, Smith KM, and Spiro TG (1993) Complete assignment of cytochrome c resonance Raman spectra via enzymatic reconstitution with isotopically labaled hemes. *J. Am. Chem. Soc.*, 115, 12446-12458.

Kagan VE, Bayir HA, Belikova NA, Kapralov O, Tyurina YY, Tyurin VA, Jiang J, Stoyanovski DA, Wipf P, Kochanek PM, Greenberger JS, Pitt B, Shvedova AA, and Borisenko G (2009) Cytochrome c/cardiolipin relations in mitochondria: a kiss of death. *Free Radic. Biol. Med.*, 46, 1439-1453.

Kagan VE, Tyurin VA, Jiang J, Tyurina YY, Ritov VB, Amoscato AA, Osipov AN, Belikova NA, Kapralov A, Kini V, Vlasova II, Zhao Q, Zou M, Di P, Svistunenko DA, Kurnikov IV, and Borisenko G (2005) Cytochrome c acts as a cardiolipin oxygenase required for release of proapoptotic factors. *Nat. Chem. Biol.*, 1, 223-232.

Karube I (1989) Micro-organism based sensors, in Turner, APF, Karube, I, and Wilson, GS (Eds.), *Biosensors: Fundamentals and Applications*, Oxford Science Publications, Oxford, 13-29.

Kinnear KT and Monbouquette HG (1993) Direct electron transfer to *Escherichia coli* fumarate reductase in self- assembled alkanethiol monolayers on gold electrodes. *Langmuir*, 9, 2255-2257.

Kranich A, Ly HK, Hildebrandt P, and Murgida DH (2008) Direct observation of the gating step in protein electron transfer: Electric-field-controlled protein dynamics. *J. Am. Chem. Soc.*, 130, 9844-9848.

Kranich A, Naumann H, Molina-Heredia FP, Moore HJ, Lee TR, Lecomte S, de la Rosa MA, Hildebrandt P, and Murgida DH (2009) Gated electron transfer of cytochrome c_6 at biomimetic interfaces: A time-resolved SERR study. *Phys. Chem. Chem. Phys.*, 11, 7390-7397.

Lal S, Grady NK, Kundu J, Levin CS, Lassiter JB, and Halas NJ (2008) Tailoring plasmonic substrates for surface enhanced spectroscopies. *Chem. Soc. Rev.*, 37, 898-911.

Ledesma GN, Murgida DH, Ly HK, Wackerbarth H, Ulstrup J, Costa AJ, and Vila AJ (2007) The met axial ligand determines the redox potential in Cu-A sites. *J. Am. Chem. Soc.*, 129, 11884-11885.

Leland C and Clark JR (1989) The enzyme electrode, in Turner, APF, Karube, I, and Wilson, GS (Eds.), *Biosensors: Fundamentals and applications*, Oxford Science Publications, Oxford, 3-12.

Love JC, Estroff LA, Kriebel JK, Nuzzo RG, and Whitesides GM (2005) Self- assembled monolayers of thiolates on metals as a form of nanotechnology. *Chem. Rev.*, 105, 1103-1169.

Mahajan M, Baumberg JJ, Russell AE, and Bartlett PN (2007) Reproducible SERRS from structured gold surfaces. *Phys. Chem. Chem. Phys.*, 9, 6016-6020.

Marcus RA (1965) On the theory of electron-transfer reactions. VI. Unified treatment for homogeneous and electrode reactions. *J. Chem. Phys.*, 43, 679-702.

Marsh D, Muller M, and Schmitt FJ (2000) Orientation of the infrared transition moments for an alfa-helix. *Biophys. J.*, 78, 2499-2510.

Murgida DH and Hildebrandt P (2001a) Heterogeneous electron transfer of cytochrome c on coated silver electrodes. Electric field effects on structure and redox potential. *J. Phys. Chem. B*, 105, 1578-1586.

Murgida DH and Hildebrandt P (2001b) Proton-coupled electron transfer of cytochrome *c*. *J. Am. Chem.Soc.*, 123, 4062-4068.

Murgida DH and Hildebrandt P (2001c) Active-site structure and dynamics of cytochrome *c* immobilized on self-assembled monolayers - a time-resolved Surface Enhanced Resonance Raman spectroscopy study. *Angew. Chem. Int. Ed.*, 40, 728-731.

Murgida DH and Hildebrandt P (2002) Electrostatic-field dependent activation energies modulate electron transfer of cytochrome *c*. *J. Phys. Chem. B,* 106, 12814-12819.

Murgida DH and Hildebrandt P (2004a) Electron-transfer processes of cytochrome *c* at interfaces. New insights by Surface Enhanced Resonance Raman Spectroscopy. *Acc. Chem. Res.,* 37, 654-661.

Murgida DH, Hildebrandt P, Wei JJ, He YF, Liu HY, and Waldeck DH (2004b) Surface-Enhanced Resonance Raman spectroscopy and electrochemical study of cytochrome c bound on electrodes through coordination with pyridinyl-terminated self-assembled monolayers. *J. Phys. Chem. B,* 108, 2261-2269.

Murgida DH and Hildebrandt P (2005) Redox and redox-coupled processes of heme proteins and enzymes at electrochemical interfaces. *Phys. Chem. Chem. Phys.,* 7, 3773-3784.

Murgida DH and Hildebrandt P (2008) Disentangling interfacial redox processes of proteins by SERR spectroscopy. *Chem. Soc. Rev.,* 37, 937-945.

Nayak S, Yeo W-S, and Mrksich M (2007) Determination of kinetic parameters for interfacial enzymatic reactions on self-assembled monolayers. *Langmuir,* 23, 5578-5583.

Paggi DA, Martin DF, Kranich A, Hildebrandt P, Marti MA, and Murgida DH (2009) Computer simulation and SERR detection of cytochrome c dynamics at SAM-coated electrodes. *Electrochim. Acta,* 54, 4963-4970.

Pereira MM and Teixeira M (2004) Proton pathways, ligand binding and dynamics of the catalytic site in haem-copper oxygen reductases: a comparison between the three families. *Biochim. Biophys. Acta,* 1655, 241-247.

Pitcher RS and Watmough NJ (2004) The bacterial cytochrome *cbb$_3$* oxidases. *Biochim. Biophys. Acta,* 1655, 388-399.

Rivas L, Murgida DH, and Hildebrandt P (2002) Conformational and redox equilibria and dynamics of cytochrome *c* immobilized on electrodes via hydrophobic interactions. *J. Phys. Chem. B,* 106, 4823-4830.

Rivas L, Soares CM, Baptista AM, Simaan J, Di Paolo R, Murgida D, and Hildebrandt P (2005) Electric-field-induced redox potential shifts of tetraheme cytochromes c$_3$ immobilized on self-assembled monolayers: Surface Enhanced Resonance Raman spectroscopy and simulation studies. *Biophys. J.,* 88, 4188-4199.

Sharma V, Puustinen A, Wikstorm M, and Laakkonen L (2006) Sequence analysis of the *cbb$_3$* oxidases and an atomic model for the *Rhodobacter sphaeroides* enzyme. *Biochemistry,* 45, 5754-5765.

Siebert F and Hildebrandt P (2008) *Vibrational Spectroscopy in Life Science.* Wiley-VCH, Weinheim

Spiro TG and Czernuszewicz R (1995) Resonance Raman spectroscopy of metalloproteins. *Methods Enzymol.,* 26, 867-876.

Todorovic S, Jung C, Hildebrandt P, and Murgida DH (2006) Conformational transitions and redox potential shifts of cytochrome P450 induced by immobilization. *J. Biol. Inorg. Chem.,* 11, 119-127.

Todorovic S, Pereira M, Bandeiras T, Teixeira M, Hildebrandt P, and Murgida DH (2005) Midpoint potentials of hemes *a* and *a$_3$* in the quinol oxidase from *Acidianus ambivalens* are inverted. *J. Am. Chem. Soc.,* 127, 13561-13566.

Todorovic S, Verissimo A, Pereira M, Teixeira M, Hildebrandt P, Zebger I, Wisitruangsakul N, and Murgida D (2008) SERR-spectroelectrochemical study of a *cbb₃* oxygen reductase in a biomimetic construct. *J. Phys. Chem. B,* 112, 16952-16959.

Ulman A (2000) Self-assembled monolayers of rigid thiols. *Rev. Mol. Biotech.,* 74, 175-188.

Ulman A (1996) Formation and structure of self-assembled monolayers. *Chem. Rev.,* 96, 1533-1554.

Veríssimo A, Sousa FL, Baptista AM, Teixeira M, and Pereira M (2007) Thermodynamic redox behavior of the heme centers of *cbb₃* heme-copper oxygen reductase from *Bradyrhizobium japonicum. Biochemistry,* 46, 13245-13253.

Wei JJ, Liu HY, Dick AR, Yamamoto H, He YF, and Waldeck DH (2002) Direct wiring of cytochrome c´s heme unit to an electrode: electrochemical study. *J. Am. Chem. Soc.,* 124, 9591-9599.

Weidinger IM, Murgida DH, Dong WF, Mohwald H, and Hildebrandt P (2006) Redox processes of cytochrome c immobilized on solid supported polyelectrolyte multilayers. *J. Phys. Chem. B,* 110, 522-529.

Willner I and Katz E (2000) Integration of layered redox proteins and conductive supports for bioelectronic applications. *Angew. Chem. Int. Ed.,* 39, 1180-1218.

Xavier AV (2004) Thermodynamic and choreographic constraints for energy transduction by cytochrome c oxidase. *Biochim. Biophys. Acta,* 1658, 23-30.

Xiao Y, Patolsky F, Katz E, Hainfeld JF, and Willner I (2003) Plugging into enzymes: nanowiring of redox enzymes by a gold nanoparticle. *Science,* 299, 1877-1881.

Yue HJ, Khoshtariya D, Waldeck DH, Grochol J, Hildebrandt P, and Murgida DH (2006) On the electron transfer mechanism between cytochrome c and metal electrodes. Evidence for dynamic control at short distances. *J. Phys. Chem. B,* 110, 19906-19913.

Zufferey R, Arslan E, Thony-Meyer L, and Hennecke H (1998) How replacement of the 12 conserved histidines of subunit I affects assembly, cofactor binding, and enzymatic activity of the *Bradyrhizobium japonicum cbb₃*-type oxidase. *J. Biol. Chem.,* 273, 6452-6459.

Zuo P, Albrecht T, Barker PD, Murgida DH, and Hildebrandt P (2009) Interfacial redox processes of cytochrome b₅₆₂. *Phys. Chem. Chem. Phys.,* 11, 7430-7436.

Biomimetics Learning from Nature

Edited by Amitava Mukherjee

ISBN 978-953-307-025-4

Hard cover, 534 pages

Publisher InTech

Published online 01, March, 2010

Published in print edition March, 2010

Nature's evolution has led to the introduction of highly efficient biological mechanisms. Imitating these mechanisms offers an enormous potential for the improvement of our day to day life. Ideally, by bio-inspiration we can get a better view of nature's capability while studying its models and adapting it for our benefit. This book takes us into the interesting world of biomimetics and describes various arenas where the technology is applied. The 25 chapters covered in this book disclose recent advances and new ideas in promoting the mechanism and applications of biomimetics.

How to reference

In order to correctly reference this scholarly work, feel free to copy and paste the following:

Daniel H. Murgida, Peter Hildebrandt and Smilja Todorovic (2010). Immobilized Redox Proteins: Mimicking Basic Features of Physiological Membranes and Interfaces, Biomimetics Learning from Nature, Amitava Mukherjee (Ed.), ISBN: 978-953-307-025-4, InTech, Available from:
http://www.intechopen.com/books/biomimetics-learning-from-nature/immobilized-redox-proteins-mimicking-basic-features-of-physiological-membranes-and-interfaces

INTECH
open science | open minds